LETTERS IN BIOMATHEMATICS
An International Journal

Intercollegiate Biomathematics Alliance

RESEARCH ARTICLE

OPEN ACCESS

Mathematical Modeling and Dynamics of SARS-CoV-2 in Colombia: Implications to Public Health Preparedness and Managing Outbreaks

Jorge H. Rojas[a], Marlio Paredes[b,c], Malay Banerjee[d], Olcay Akman[e], Anuj Mubayi[e]

[a]Epidemiology and Public Health in Promotion, Prevention and Social Production of Health SubSecretary, Public Health Secretary of Mayor Cali, Colombia; [b]Department of Mathematics, Universidad del Valle, Cali, Colombia; [c]Institute of Science, Technology and Innovation, Universidad Francisco Gavidia, San Salvador, El Salvador; [d]Department of Mathematics and Statistics, Indian Institute of Technology, Kanpur, India; [e]Center for collaborative Studies in Mathematical Biology, Illinois State University, Normal, USA

ABSTRACT

As COVID-19 continues to spread around the globe, it is critical to understand the true burden of a future outbreak in developing countries like Colombia where data may be limited. Here, we estimated the rate of the initial exponential growth of cases and the basic reproductive rate for the disease. We use models with different modeling assumptions to study the differences between five major Colombian cities and between selected Latin American countries. Using an ensemble modeling technique, we estimated that the reproduction number in Colombia varied from 1.10 in Cartagena to 1.75 in Medellin with Cali being 1.47. In Latin America, Ecuador has highest initial epidemic growth rate and Panama the lowest with Colombia in middle of the list. The choice of appropriate model and parameter estimates for a location provided different scenarios in outbreaks. This analysis provides a framework for the decision makers to be better prepared for an outbreak.

ARTICLE HISTORY
Received May 5, 2020
Accepted April 26, 2022

KEYWORDS
coronavirus outbreak, dynamical model, epidemic burden, basic reproduction number, exponential initial rise in new cases

1 Introduction

An outbreak of pneumonia with unknown etiology in the Wuhan city, Hubei's province in Mainland China was first reported on December 31, 2019 by the World Health Organization (WHO). On January 7, 2020 a virus associated with this outbreak was isolated (Minwang et al., 2020) and found to be novel strain of Coronavirus that may have crossed over to human population from its sylvatic host. On January 30, 2020, WHO declared the Public Health emergency of International importance (OMS, 2020) and denominated this coronavirus as SARS-COV-2 while the disease was referred as COVID-19 on February 12, 2020 (Figueroa, 2020). This virus belongs to the genus betacoronavirus of the subfamily coronavirus and family Coronaviridae. The 2002–2004 SARS epidemic and the 2012–2016 MERS epidemic were also caused by the viruses belonging to the family coronavirus; however, both showed lower transmissibility and absolute lethality (Chen, 2020).

In order to protect people from this unknown outbreak of COVID-19 it is critical to understand its trends and estimate potential burden. Mathematical models have been used before to this purpose for various epidemic diseases and can be extremely helpful in disease preparedness. An important threshold quantity associated with a disease transmissibility is the basic reproduction number, denoted by R_0 (pronounced "R naught"). The epidemiological definition of R_0 is the average number of new cases of the disease that will be generated by one contagious person during his/her infectious period. It specifically applies to a population of people who were previously free of infection and not vaccinated. Three possibilities exist for the potential spread or decline of a disease, depending on its R_0 value: (i) If R_0 is less than 1, each existing infection causes less than 1 new infection. In this case, the disease will decline and eventually disappear. (ii) If R_0 equals 1, the disease will stay alive, but there won't be an epidemic. (iii) If R_0 is greater than 1, cases could grow exponentially and cause an epidemic or even a pandemic (Brauer and Castillo-Chavez, 2012) . A preliminary R_0 estimate of 1.4–2.5 was presented on Jan 23, 2020 in a WHO statement regarding the outbreak of 2019-nCoV (Minwang et al., 2020). Zhao et al. (2020) estimated the mean R_0 for 2019-nCoV in the early phase of the outbreak ranging from 3.3 to 5.5 (likely to be below 5 but above 3 with rising report rate) (Zhao et al., 2020; Chaolin

CONTACT Anuj Mubayi amubayi@asu.edu

et al., 2020), which appeared slightly higher than those of SARS-CoV (R_0:2-5) (Chen, 2020). Read et al. (2020) estimated the R_0 for 2019-nCoV to be in the range 3.6–4.0, indicating that 72–75% of transmissions must be prevented in order to stop the increasing trend. The explosive and dramatic behavior of the spread of this virus SARS-CoV-2 in mainland China, has forced health and administrative authorities take severe and strict control measures. Until January 31, 2020, 11,950 cases had been reported and 259 deaths but the number of cases had increased to 75,184 and 2009 deaths on February 18, 2020 (COVID-19, 2020). The pharmacological treatment with antivirals is unknown and the vaccine is in the early stages of investigation.

The major cities of Colombia are Cali, Bogota, Barranquilla, Cartagena, and Medellin with population size 2.5M, 7.2M, 1.2M, 0.9M, and 2.6M, respectively. Climatic conditions remains almost similar between cities but socio-economic characteristics varies tremendously between them. In these cities, more than 98% of population lives in urban areas (Escobar and Perilla, 2019), with an average temperature of about 24°C, an annual precipitation of more than 1,000 mm. The weather in these cities has two seasons including a dry season (from December to January and July to August) and a cloudy season (from April to May and October to November). Some strains of Coronavirus may be related to climatic conditions with colder weather more suitable for their spread. Many of these cities are touristic city and the number of passengers moved by international routes in Colombia (Aeronáutica, 2020) reached more than 11M people alone in the first half-year. COVID-19 surveillance data is considered weak in many areas of Colombia. There are various intervention programs to control COVID-19 outbreaks are in place in Colombia. However, there remains significant challenges such limited resources available for Colombia's surveillance system and the national laboratory network. Moreover, public health educational programs to make public aware of self-protection measures need to be strengthen in order to quickly mitigate the impact of the disease. Between the factors (Oaks et al., 1992) explain the emergence or re-emergence of infectious diseases the modern aeronautical technology allows the connection between countries in very short time and thus sick people carry infectious agents over long distances (Anaya, 2017). This information will allow prepare plans of education to community that interrupts the transmission of the virus. Coronavirus has been in Latin America since February of 2020. Since then countries across the region have implemented various social distancing and lockdown policies to control the COVID-19 pandemic, with varied success.

The objectives of this study are to (i) use available current COVID-19 information and estimate via showcasing ensemble modeling technique, for Colombia, the disease burden under different modeling assumptions, and (ii) compare situation in five major cities of Colombia, and (iii) compare the situation in Colombia with other similar Latin American countries.

2 Materials and Methods

We considered different modeling assumptions to capture COVID-19 outbreak in five major cities of Colombia and selected Latin American countries. In order to understand the ongoing burden of the disease, a systematic procedure was implemented. The procedure in this study primarily involves four steps: (i) Using reported estimates of R_0 and model-derived formulation of R_0 (corresponding to different model and under the assumption of initial exponential growth rate of epidemic), estimate effective transmission rate in the population, (ii) Use estimated effective transmission rate, demographic data from cities of Colombia and epidemic models, to predict different outbreak scenarios for cities, and (iii) From these outbreak scenarios (in step (ii)), estimate the disease burden.

2.1 Basic modeling framework

Mathematical model to capture a potential outbreak. For the mathematical modeling of the transmission dynamics of the new SARS-CoV-2 coronavirus, we have established the structure compartmental of SEIR model (Susceptible, Exposed, Infectious, Recovered) and applying the method of differential equations based on the COVID-19 epidemic data in continental China (Li et al., 2020; Vynnycky and White, 2010).

$$\begin{aligned}
\frac{dS(t)}{dt} &= -\lambda(t)S(t)\\
\frac{dE(t)}{dt} &= \lambda(t)S(t) - fE(t)\\
\frac{dS(t)}{dt} &= fE(t) - rI(t)\\
\frac{dS(t)}{dt} &= rI(t)
\end{aligned} \tag{1}$$

Model variables and parameters are defined in Table 1. The rest of the models are defined in Table 3 and in the Supplementary Material, section B.

Table 1: Variables and parameters of the SEIR model.

	Symbol	Definition
Variables	S	Susceptible population
	E	Exposed (pre-infectious) population
	I	Infectious population
	R	Recovered population
Parameters	λ	Rate at which susceptible individuals becoming infected per unit time, at time t
	f	Rate at which individuals in the pre-infectious category become infectious per unit time
	r	Rate at which infectious individuals recover per unit time

Model-related metrics. Consider a simple epidemic model, Susceptible-Infectious-Recovered (SIR) or Susceptible-Exposed-Infectious-Recovered (SEIR) model with I individuals are only infectious. The number of susceptible individuals who are infected per unit time is given by the product of the force of infection, $\lambda(t)$, and the number of susceptible individuals at time t (i.e., $\lambda(t)(t)S(t)$) under the assumption that individuals contact each other randomly. Let $\lambda(t)$ be the force of infection or rate at which a susceptible individual is infected or rate at which they move to an infected compartment then it can be written as

$$\lambda(t) = \beta I(t) \tag{2}$$

where β is the rate at which two specific individuals come into effective contact per unit time and $I(t)$ is the number of infectious individuals at time t. The formula for basic reproduction number of the model is $R_0 = \beta ND$ and can used it to estimate effective contact rate as

$$\beta = \frac{R_0}{ND} \tag{3}$$

where N is the population size at the beginning of an outbreak and D is the length of the infectious period.

Now if Exposed state (defined as individuals who are infected not infectious) is present in the model then the model will be referred as SEIR model. Suppose f is the rate at which the individuals move from exposed compartment to infectious compartment. The rate $f = 1/D'$, where D' is the duration of the latent or pre infectious period. Let r be the rate at which the individuals move from infectious compartment to recovered or immune compartment, i.e., $r = 1/D$, where D is the duration of the infectious period.

Since R_0 is a metric computed early in the epidemic, it can be used to relate it with the initial growth rate of an epidemic. Different formulae are used to estimate R_0 using data from the early stages of an epidemic, each of them requires estimates of something which is often referred to as exponential growth of rate of the epidemic sometimes denoted by Λ (capital lambda). During the early stages of an epidemic, the number of infectious individuals increases at an approximately constant exponential growth rate.

2.2 Estimation of various relevant quantities

Initial exponential growth rate. We can estimate this growth rate as follows. Consider an exponential growing function of number of reported cases $I(t)$ where Λ is the exponential growth rate parameter, i.e.,

$$I(t) = I(0)e^{\Lambda t} \tag{4}$$

where $I(0)$ is the initial number of infectious individuals at the beginning of infection. If we take natural logarithm of this equation, we obtain the following equation:

$$\ln(I(t)) = \ln(I(0)) + \Lambda t \tag{5}$$

relating the number of infectious individuals and Λ. Note, this is the equation of a straight line with slope Λ, suggesting that if we plot the natural logarithm of the number of infectious individuals against time, we should obtain a straight line with slope Λ.

On the other hand, we can also write an expression of R_0, in terms of Λ. This expression of R_0 will depend on the type of model considered and other model parameters including D' and D the average durations of the pre-infectious and infectious periods respectively. Sometimes R_0 can also be expressed in terms of the serial interval, T_s (defined as the time between the start of symptoms in the primary patient (infector) and onset of symptoms in the patient receiving that infection from the infector (the infected) (Chaolin et al., 2020). In Table 3 the different formulas are shown. For example, in case of the SEIR model with only I infectious, the basic reproduction number can be written as

$$R_0 = (1 + \Lambda D)(1 + \Lambda D') \tag{6}$$

and in case of the SIR model, $R_0 = 1 + \Lambda D$.

Furthermore, we can use equation (5) to obtain the relationship between the growth rate Λ and the doubling time T_d of an epidemic, which is defined as the time until the number of cases in the population doubles, relative to that at some other time. Suppose that there is only one infectious individual at time $t = 0$ (i.e., $I(0) = 1$) and there are two infectious individuals at time $t = T_d$ (i.e., $I(T_d) = 2$). Substituting for $I(0) = 1$ and $I(T_d) = 2$ into equation (5) we obtain $\ln 2 = \ln 1 + \Lambda T_d$ which implies

$$\Lambda = \frac{\ln 2}{T_d} \tag{7}$$

Since R_0 can be written in the form of Λ and the doubling time can be computed as in equation (7), we can find T_d in terms of R_0. For example, in case of SIR model,

$$T_d = \frac{(\ln 2) \cdot D}{R_0 - 1} \tag{8}$$

and in case of SEIR model with only I infectious, it can be written as

$$T_d = \frac{\ln 2}{\tilde{\Lambda}} \tag{9}$$

where $\tilde{\Lambda} = \left(-D_1 + \sqrt{D_1^2 + 4(R_0 - 1)D_2}\right)/(2D_2)$, $D_1 = D + D'$, and $D_2 = D \cdot D'$. This formula can be used to study the role of epidemiological factors such as transmission rate (β), asymptomatic and symptomatic periods.

Estimation of model parameters. In groups of Japanese migrants who were repatriated, the proportion of positive asymptomatics to PCR test, was estimated by Nishiura et al. (2020) in 41.6% (CI 95%: 16.7–66.7); Kimball et al. (2020) found 57%; and Mizumoto et al. (2020) 51.7%. For purpose of our study we will take 50% as parameter value (Chen et al., 2020). It has also been established that 14% of the symptomatic people are hospitalized for complications related to pneumonia and respiratory distress (CDC, 2020; Wu and McGoogan, 2020). From those hospitalized, 15% die (Huang et al., 2020; MSE, 2020; Wang et al., 2020). Because COVID-19 is a novel disease, some parameters are unknown or are known with less precision, and hence, they are estimated. Using case reports, outbreaks' studies and some based on the behavior of coronavirus in past epidemics, these parameters are estimated. Multiple research articles report incubation period estimates obtained from different methods. The most of them report incubation period mean between 5–7 days and the range between 2–14 days (González-Jaramillo et al., 2020; Liu et al., 2020; Imai et al., 2020; Backer et al., 2020; Ganyani et al., 2020; Guan et al., 2020; Adhikari et al., 2020; Zheng, 2020; Lauer et al., 2020). We have used the incubation period to be 6.4 days based on most of the studies. Although the virus SARS-2 can be detected in nasopharyngeal swab between 2.5 days before and 18 days after starting symptoms, infectivity is considered very low after 7 days. The infectious period is assumed for this study, an average of 7.6 days based on reported 14 days quarantine period COVID-19 (Hu et al., 2020; Murcia, 2020; Ministerio, 2020; Tan et al., 2020; He et al., 2020).

Estimation of R_0. The data used for calculating R_0 were collected from published research (for example, (Li et al., 2020)). The novel coronavirus SARS-CoV-2, causes COVID-19, which is characterized mainly by fever, muscle pain and cough and it can move along to severe phases of pneumonia or even die. Because it is a new disease, there is a small knowledge about the time of latent period, infectious period in the natural history of disease, though some estimates have been made based on cluster of cases and hospitalized.

2.3 Models

In this study, we consider various modeling assumptions leading to six different models defined in Table 2, Table 3 and their details are given in Supplementary Material. An additional (seventh) model, referred to as Age of Infection model (details of which are given in Supplementary Material Section C), is not used in the main text for estimation of parameters for COVID-19 in Colombia, but some mathematical details are mentioned in Supplementary Material for future application. Suppose S, E, I, R, T, J, Q_1, Q_2 and Q_3 represent Susceptible, Exposed, Infectious, Recovered, Treated, Hospitalized, Susceptible-Quarantined, Exposed-Quarantined and Infectious-Isolated (Table 2). The models are

Model I: simple SIR,
Model II: simple SEIR with I only infectious,
Model III: simple SEIR with E and I infectious,
Model IV: SITR,
Model V: SEIR-Q1Q2Q3,
Model VI: SEIJR.

Table 2: Definition of state variables in the six models and corresponding models in which they are used.

Symbol	Definition	Model #
S	Susceptible	I–VI
E	Exposed	II, III, V, VI
I	Infectious	I–VI
R	Recovered	I–VI
T	Treated	IV
J	Hospitalized	VI
Q_1	Susceptible-Quarantined	V
Q_2	Exposed-Quarantined	V
Q_3	Infectious-Isolated	V

3 Ensemble Forecast

Ensemble forecasting, a primary method in climate modeling, is used to improve predictions of disease burden for relatively longer time. It is also helpful in providing range of potential outcomes and requires large amount of data for parameterization and validation. For example, predictions and projections of weather and climate from time scales of days to decades are considered using simulations of models that captures uncertainties in the initial condition, boundary condition, model parameters and model structural uncertainties. In climate modeling, initial condition uncertainty is most relevant for the shortest time scales; whereas, long-term projections of climate often require averaging across several ensemble members. The focus of the ensemble forecasting method is to improve performance of any one individual model or reduce the probability of choosing a single poor model from a set. In the method, multiple models with independent projections are combined, resulting in one improved model to guide decision-making. The multiple models can simply differ from each other in structure (i.e., models vary between assumptions on epidemiology) or alternatively can use single structure of a model but take into account changes in its parameters (including initial conditions) over its reasonable range of values to produce a set of different results. Once different results from the models are created, the results are then averaged by using some weighting schemes, which could range from simple linear combination to sophisticated non-linear averaging.

3.1 Model choices and assumptions

In general, because the true disease system is highly complex, it remains fundamentally impossible to describe all its processes in an epidemic model. Hence, modelers often make choices in selecting relevant processes, which directly depend on the question of interest. Uncertainty that is introduced by choices in the model design and not by changing parameter values, is called as structural uncertainty. In this study, we give an example of how structural uncertainty is applied for the infectious disease system such as tracking COVID-19 pandemic. There are different ways to combine models in a multi-models ensembles. Models weighted averages, where weights are determined by using the error relationship between model forecasts and observations, perform better than simple averages. In the present study, we assess the potential for uncertainties about SARS-CoV-2 virus that impact forecasts of the disease spread. In order to achieve our goals, we evaluated the performance of six simple forecasting models in the context of the COVID-19 pandemic in cites of Colombia. Each of the models have different features representing a different combination of assumptions about epidemiology of pathogen, variation in transmission potential, and stages of infection. The outcomes of the study include identification of the model assumptions that had the most ensemble weight changed through time, evaluation of a trade-off when some individual models outperformed ensemble models early in the epidemic, but on average the ensembles outperformed all individual models, and stresses that multiple models capturing uncertainty across alternative assumptions are necessary to obtain robust forecasts for diseases such as COVID-19 in a developing country like Colombia where there may substantial delay in data reporting and data might be incomplete in some instances.

3.2 Types of weighting scheme

The first type of averaging in the multi-model ensemble includes weighting all members by equal weight. In this case, averaging is referred to as a "model democracy" (models in the ensemble are independent and equally plausible). The second type assumes independent members but some have higher weights than others. In this weights are defined using formula $\exp(-D_i/\sigma_D^2)$, where D_i represents the RMSE distance between a multi-model ensemble member and observations, and σ_D^2 determines how far apart a member and observations must be to be down-weighted. There are different ways in which weights can be computed.

Table 3: Formulas to the basic reproduction number estimates.

R_0 or R_c in terms of Λ	Assumptions	Model (Actual R_0 or R_c)
$1 + \Lambda D$	This expression assumes that the pre-infectious period is very short in comparison with the infectious period, or individuals are infectious immediately after they are infected. The infectious period is assumed to follow the exponential distribution. (Supplementary Material, section B.1)	SIR $\left(R_0 = \frac{\beta N}{\alpha}\right)$ Model I, Eq. B1, Fig. B1, Table B1, (Brauer, 2010)
$(1 + \Lambda D)(1 + \Lambda D')$	The pre-infectious and infectious periods follow the exponential distribution. Neither the pre-infectious nor infectious periods are short, relative to the other. (Supplementary Material, section B.2)	SEIR with only I Infectious $\left(R_0 = \frac{\beta N}{\alpha}\right)$ Model II, Eq. B6, Fig. B2, Table B2, (Brauer, 2010)
$(1 + \Lambda D')(1 + \Lambda D)\left(1 + \frac{1}{DD'\varepsilon}\right)\left(\frac{1}{1+\Lambda D+\frac{1}{DD'\varepsilon}}\right)$	It is assumed that E individuals are infectious and transmit infection, however, their infectivity is lower than that of I individuals. (Supplementary Material, section B.3)	SEIR with E & I infectious $\left(R_0 = \frac{\beta N}{\alpha} + \frac{\varepsilon\beta N}{\kappa}\right)$ Model III, Eq. B10, Fig. B3, Table B3, (Brauer, 2010)
$\frac{(\eta + \delta\gamma)(\Lambda + \eta)(\Lambda + \alpha + \gamma)}{\eta(\alpha + \gamma)(\Lambda + \eta + \delta\gamma)}$	It assumes that there is no E stage (i.e., no asymptomatic stage) but there are some therapeutic effects on patients in isolation. (Supplementary Material, section B.4)	SITR model with treatment $\left(R_0 = \frac{\beta N}{\alpha+\gamma}\left(1 + \frac{\delta\gamma}{\eta}\right)\right)$ Model IV, Eq. B14, Fig. B4, Table B4, (Brauer, 2010)
$\frac{\left(\sigma + \alpha_1 + \frac{\gamma_1}{q}\right)(\Lambda + \sigma + \alpha_1)(\Lambda + \gamma_1 + \phi)}{(\gamma_1 + \phi)(\sigma + \alpha_1)\left(\Lambda + \sigma + \alpha_1 + \frac{\gamma_1}{q}\right)}$	It assumes SEIR type model but with quarantining for suspected cases and isolation for confirmed cases due to these measures. (Supplementary Material, section B.5)	SEIR-Q1Q2Q3 model with standard incidence $\left(R_c = \frac{\beta q}{\gamma_1+\phi} + \frac{\beta\gamma_1}{(\gamma_1+\phi)(\sigma+\alpha_1)}\right)$ Model V, Eq. B18, Fig. B5, Table B5
$\frac{\Delta(\Lambda + \eta + \tau + \mu)(\Lambda + \alpha_1 + \sigma + \delta)(\Lambda + \alpha_2 + \delta)}{\tilde{q}(\Lambda + \alpha_1 + \sigma + \delta)(\Lambda + \alpha_2 + \delta) + \tau(\Lambda + \alpha_1 + \sigma + \delta) + l(\eta(\Lambda + \alpha_1 + \sigma + \delta) + \tau\sigma)}$	It assumes that hospitalization of individuals is possible quickly and asymptomatic/symptomatic both are infectious. (Supplementary Material, section B.6)	SEIJR model with standard incidence $\left(R_c = \frac{\beta q}{\eta+\kappa+\mu} + \frac{\beta\kappa}{(\eta+\kappa+\mu)(\gamma_1+\alpha+\delta)} + \frac{\beta l(\alpha\eta+\alpha\kappa+\eta\delta+\gamma_1\eta)}{(\eta+\kappa+\mu)(\gamma_1+\alpha+\delta)(\gamma_2+\delta)}\right)$ Model VI, Eq. B22, Fig. B6, Table B6

Table 4: Category of analysis based on model assumptions.

Models with no interventions	Models with treatment	Models with prevention
SIR (Model I)	SITR (Model IV)	SEIR-Q1Q2Q3 (Model V)
SIER with I infectious (Model II)	SEIR-Q1Q2Q3 (Model V)	SEIJR (Model VI)
SEIR with E&I infectious (Model III)	SEIJR (Model VI)	

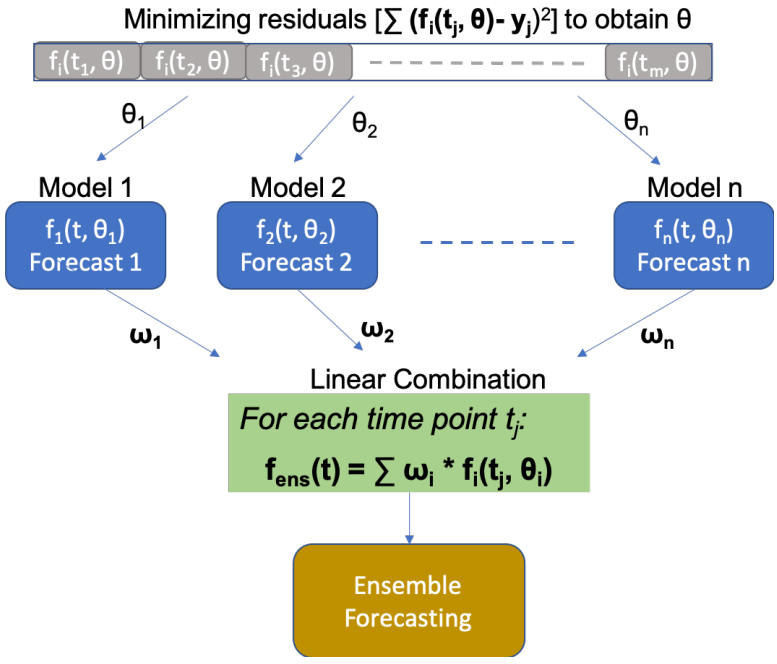

Figure 1: Steps in ensemble method.

Table 5: Parameter estimates of the six models.

Parameter	Description	Value and units	References
	Model I: SIR model		
β_1	Transmission rate	6.47×10^{-9} day^{-1}	Estimated
α	Infectious period (14 days)	0.0714 day^{-1}	Chaolin et al., 2020; Kimball et al., 2020
	Model II: SEIR model		
β_2	Transmission rate	1.79×10^{-8} day^{-1}	Estimated
κ	Pre-infectious period (5.2 days)	0.1923 day^{-1}	Li et al., 2020
α	Symptomatic infectious period (7 days)	0.143 day^{-1}	Chaolin et al., 2020; Kimball et al., 2020
	Model III: SEIR model with infectivity in exposed stage		
β_3	Transmission rate	3.5×10^{-10} day^{-1}	Brauer and Castillo-Chavez, 2012; Li et al., 2020
κ	Asymptomatic latent period (5.2 days)	0.1923 day^{-1}	Li et al., 2020
ε	Relative transmissibility reduction of E	0.5 day^{-1}	Chaolin et al., 2020
α	Symptomatic infectious period (7 days)	0.143 day^{-1}	Chaolin et al., 2020; Kimball et al., 2020
	Model IV: SIR model with treatment		
β_4	Transmission rate	1.06×10^{-8} day^{-1}	Estimated
ρ	Reduce infectivity of T class individuals	0.3 day^{-1}	Orellana et al., 2020
σ	Per capita isolation rate at symptomatics	0.1639 day^{-1}	Kucharski et al., 2020
α_1	Recovery rate	0.1809 day^{-1}	Kucharski et al., 2020; Liu et al., 2020
α_2	Recovery rate among treated	0.1061 day^{-1}	Ivorra et al., 2020
	Model V: SEIR model with quarantine and isolation		
β_5	Transmission rate	0.79	Estimated
ϕ	Per capita quarantine rate	0.20 day^{-1}	Mubayi et al., 2010
$1/\theta$	Average time in quarantine	6 (days)	Mubayi et al., 2010
q	Reduce infectivity of E class individual	0.5	Assumed (varied)
γ_1	Per capita recovery rate of symptomatics	0.125 day^{-1}	Wei et al., 2020
γ_2	Per capita recovery rate among hospitalized	0.75 day^{-1}	Wei et al., 2020
σ	Per capita isolation rate of symptomatics	0.1639 day^{-1}	Kucharski et al., 2020
α_1	Per capita recovery rate of symptomatics	0.1809 day^{-1}	Kucharski et al., 2020; Liu et al., 2020
α_2	Recovery rate among treated	0.1061 day^{-1}	Ivorra et al., 2020
	Model VI: SEIR model with hospitalization and exposed infectiousness		
β_6	Transmission rate	2.83×10^{-7} day^{-1}	Estimated
$\tilde{q}$	Reduce infectivity of E class individual	0.5	Assumed (varied)
l	Reduced infectivity of J individual	0.4	Assumed (varied)
τ	Pre-infectious period (assumed same as η)	0.85 day^{-1}	Escobar and Perilla, 2019
μ	Per capita recovery rate of asymptotics	0.2 day^{-1}	Wei et al., 2020
η	Recovery rate among treated	0.85 day^{-1}	Escobar and Perilla, 2019
α_1	Per capita recovery rate of symptomatics	0.1809 day^{-1}	Kucharski et al., 2020; Liu et al., 2020
α_2	Recovery rate in treated: the rate at which the infectious are treated and cured	0.1061 day^{-1}	Ivorra et al., 2020
σ	Per capita isolation rate of symptomatics	0.1639 day^{-1}	Kucharski et al., 2020
δ	Per capita disease related mortality rate	0.025 day^{-1}	Wei et al., 2020

Table 6: Date of reporting starts and first exponential day.

Country	Date of reporting starts	Estimated date of first Case (number of days of delay)	Initial reported cases $y(0)$	Λ	R-squared
South Africa	03/09/2020	03/04/2020 (5 days)	4	0.3105	0.98
South Korea	02/19/2020	02/03/2020 (16 days)	86	0.2861	0.89
Ecuador	03/13/2020	03/01/2020 (12 days)	21	0.2618	0.86
Chile	03/10/2020	02/28/2020 (11 days)	14	0.2473	0.92
Brazil	03/10/2020	02/24/2020 (15 days)	36	0.2419	0.93
Mexico	03/11/2020	03/02/2020 (9 days)	8	0.2418	0.92
Colombia	03/09/2020	03/02/2020 (7 days)	5	0.2391	0.92
Peru	03/09/2020	02/28/2020 (10 days)	8	0.2231	0.89
Argentina	03/09/2020	03/28/2020 (10 days)	8	0.2158	0.96
Panama	03/11/2020	02/25/2020 (15 days)	18	0.2056	0.95

4 Results

We assume that the initial (at starting time) values of the state variables in the models are $I_0 = 1, S_0 = N - I_0$ and other state variables were taken as zero. The parameter estimates of the models were collected in Table 5, in Table 7, and in Supplementary Material Tables B1–B6.

4.1 Initial exponential growth rate

Exponential growth model was used to estimate initial exponential growth rate in a city. The exponential function (Equation (4) or (5)) is fitted to reported cases from different countries. For example, the early estimated growth rate using data from China is found to around 0.17 (Figure A1, Supplementary Material) with the confidence interval given by 95% CI $(0.162, 0.185)$. The comparison of different exponential growth and estimated start of epidemics in some countries are computed and presented in order in the Table 6 with Colombia having estimate of 0.23. We estimated that there was a delay of approximately 7 days in the first reported case by Colombia. Among the 10 countries considered here, South Africa has the highest initial exponential epidemic growth rate (0.3105) and Panama has the lowest (0.2056).

4.2 Computation of R_0 and β estimates for Colombia and its five different cities for six different models

We first computed the initial exponential growth rate (Λ) for each of the 5 major cities of Colombia. Using this Λ estimate, we then computed R_0 estimate (via formulas in Table 3), followed by corresponding β_i estimates for all six models. The estimated values are shown in Table 7.

4.3 Compare outbreaks in Colombia and its five different cities for six different models

We simulated all six models for whole Colombia and its five major cities. We computed for each model and region, the expected number of cases that needs to be hospitalized over an outbreak, maximum daily number of cases that can be expected, time needed to reach different epidemic peak and mean duration of an epidemic for the current outbreak. The simulated curve was used to compute error between observed incidence and model-estimated incidence for each region. This error was referred as "rss."

4.4 Averaging results of six different models for Colombia

The weighted average using the results from the six models was computed similar to climate models. We used AIC to estimate this weight by

$$AIC = m * \log(rss) + 2K$$

Table 7: Beta values and R_0 for five Colombian cities and six different models. First day of outbreak considered as: 05/01/2020, last day: 07/28/2020, except for Medellin which are First day: 06/01/2020, last day: 08/28/2020.

		Cali	Bogota	Barranquilla	Cartagena	Medellin
Model I	β_1	4.57×10^{-8}	1.53×10^{-8}	9.36×10^{-8}	$9.39x10^{-8}$	4.78×10^{-8}
	R_0	**1.47**	1.54	1.57	1.32	1.74
Model II	β_2	9.02×10^{-8}	3.02×10^{-8}	1.86×10^{-7}	1.85×10^{-7}	9.61×10^{-8}
	R_0	1.45	1.52	1.56	1.29	**1.75**
Model III	β_3	3.74×10^{-9}	1.76×10^{-8}	7.42×10^{-9}	8.16×10^{-9}	3.61×10^{-9}
	R_0	1.19	**1.21**	**1.23**	1.12	1.29
Model IV	β_4	1.22×10^{-7}	3.97×10^{-8}	2.41×10^{-7}	2.66×10^{-7}	1.17×10^{-7}
	R_0	1.19	1.21	1.23	1.13	1.29
Model V	β_5	0.43	0.44	0.44	0.41	0.46
	R_c	1.15	1.17	1.18	**1.10**	1.23
Model VI	β_6	0.13	0.14	0.14	0.12	0.16
	R_c	1.19	1.24	1.27	1.06	1.41

where K is the number of parameters in the model, m is sample size of the data, and rss is the ratio of the residual sum of squares = RSS/m where RSS is residual sum of squares. For small sample sizes (m/K < 40), use the second-order AIC:

$$AICc = m * \log(rss) + 2K + (2K(K+1)/(m-K-1))$$

Akaike weights (ω_i) are the weight of evidence in favor of model i being the actual best model for the situation at hand given that one of the n models must be the best model for that set of n models.

$$\omega_i = \frac{\exp\{-0.5\Delta_i\}}{\sum_{r=1}^{n} \exp\{-0.5\Delta_r\}} \tag{10}$$

where $\Delta_i = AIC_i - AIC_{min}$. Note, Akaike weights for all models combined should add up to 1. Other studies have also used weights as follows:

$$\omega_i = \frac{mse_i}{\sum_{r=1}^{n} mse_r} \tag{11}$$

where $mse_i = \frac{1}{MSE_i}$ and $MSE_i = \frac{1}{m}\sum_{j=1}^{m}(f_i(t_j, \Theta_i) - y_{t_j})^2$. Hence, the estimated mean incidence curve from the ensemble model is

$$f_{ens}(t) = \sum_{i=1}^{6} \omega_i * f_i(t_j, \Theta_i)$$

Before any weighting of results from all the models, we initially evaluated forecasting from each of the six models separately, which show very high incidence across most cities over the about 2-year period of our analysis. It seems short-term forecasts over a 2-week time horizon were consistent with the high observed incidence at that time. Over the first 12 weeks, model parameters changed modestly and correlations among parameters began to emerge. Many of the models showed only one peak unlike the observed time series where there were a few valley and peak. This may be due to choice of simple models in our set and long term fitting using the same model.

Starting the first reported case in a region, we updated parameter estimates every week, and generated forecasts every four weeks. The model-specific forecast was also quantified over time. The role of various model assumptions was incorporated into how weights of ensemble for each forecasting period was computed (three types of assumptions were considered: models with no interventions, models with treatment, and models with prevention). We summed and then normalized models' ensemble weights across each class of assumption. Table 8 provides parameters that were estimated in each of the six models.

The averaging of the ensemble models was based on AIC criteria (Table 9) and weights were computed as shown in Table 10. The model with least AIC value or highest weight are shown as bolded text in the two tables. The final averaged model of the ensemble of six models for each city is shown in the Figure 2 and Figure 3. According to the averaged ensemble model, peak in outbreak occurred during Nov-30-2020 in Cali (9928 cases), Oct-31-2020 in Bogota (38328 cases), Nov-27-2020 in Barranquilla (6918 cases), Mar-5-2021 in Cartagena (2106 cases; peak was not yet obtained in this forecast) and Oct-16-2020 in Medellin (21348 cases). This is based on the data from Mar-6-2020 to Oct-28-2020, considered in this study. The models forecasted outcomes from Oct-29-2020 to Mar-5-2021. The forecast in the averaged ensemble model were much higher in

Table 8: Parameters estimated in the respective models.

Model	Parameters		
I	β_1		
II	β_2		
III	β_3		
IV	β_4	ρ	
V	β_5	q	
VI	β_6	$\tilde{q}$	l

Table 9: AIC values for the six models for each of the five cities.

Model	Cali	Bogota	Barranquilla	Cartagena	Medellin
I	**1403.29**	1695.82	1343.04	1210.38	1160.87
II	1416.93	1701.09	1348.68	1209.35	**1159.21**
III	1580.99	**1610.42**	**1326.81**	1220.20	1193.68
IV	1503.95	1748.72	1388.94	1205.26	1178.03
V	1460.87	1709.07	1363.79	**1203.05**	1163.04
VI	2031.72	2211.06	1329.49	1223.07	1192.29

Table 10: The weights (ω) for corresponding models in the ensemble for each of the five cities.

Model	Cali	Bogota	Barranquilla	Cartagena	Medellin
I	**0.98**	2.85×10^{-19}	2.36×10^{-4}	0.02	0.27
II	0.01	2.05×10^{-20}	1.41×10^{-5}	0.03	**0.63**
III	2.59×10^{-39}	**0.98**	**0.79**	1.34×10^{-4}	2.06×10^{-8}
IV	1.38×10^{-22}	9.29×10^{-31}	2.55×10^{-14}	0.23	5.17×10^{-5}
V	3.14×10^{-13}	3.79×10^{-22}	7.36×10^{-9}	**0.71**	0.09
VI	3.45×10^{-137}	3.74×10^{-131}	0.21	3.21×10^{-5}	4.13×10^{-8}
Total	1	1	1	1	1

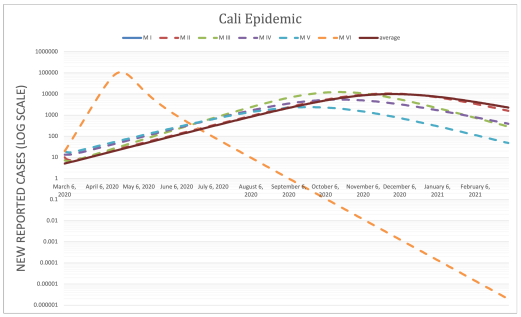

(a) Six fitted models and average ensemble for city of Cali

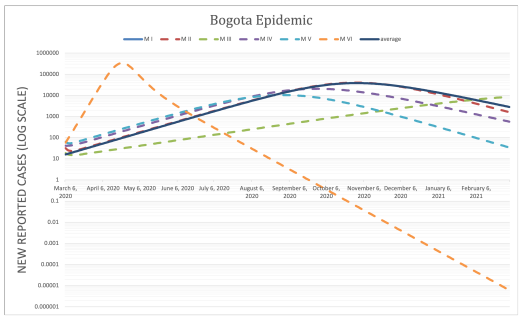

(b) Six fitted models and average ensemble for city of Bogota

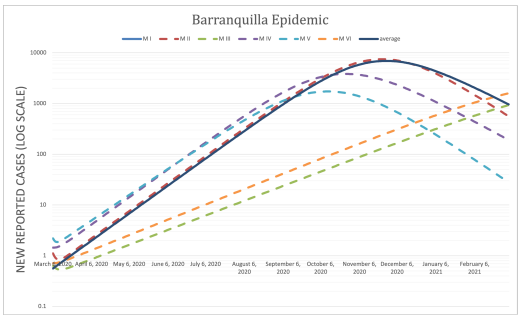

(c) Six fitted models and average ensemble for city of Barranquilla

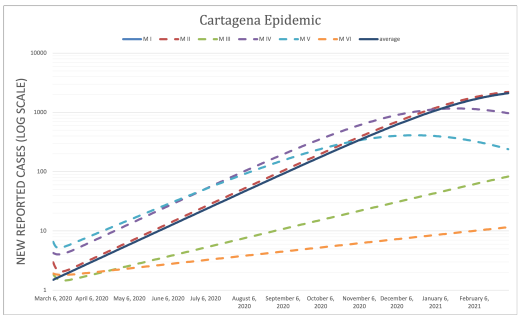

(d) Six fitted models and average ensemble for city of Cartagena

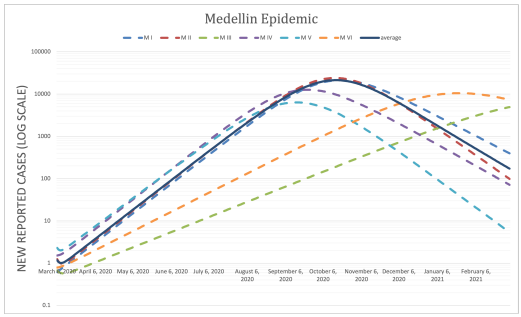

(e) Six fitted models and average ensemble for city of Medellin

Figure 2: Comparison between six models and its average ensemble model.

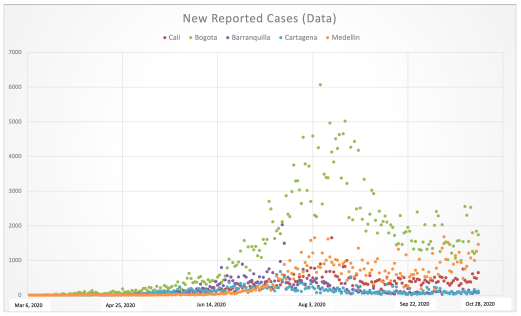

(a) Reported data from five cities to which models are fitted

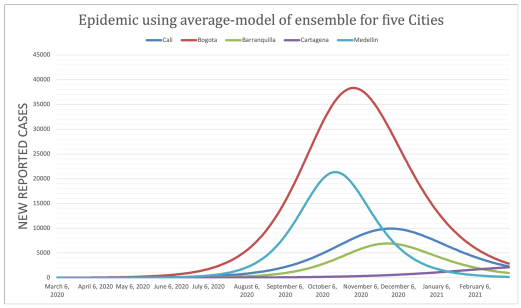

(b) Averaged ensemble model from five cities

Figure 3: Comparison fitted ensemble model with raw data.

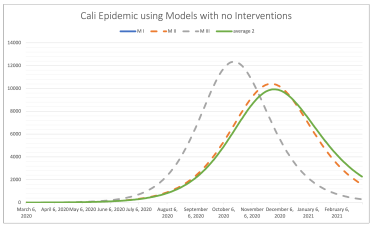

(a) Cali model forecast

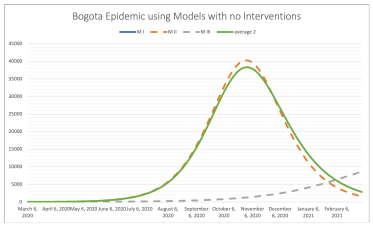

(b) Bogota model forecast

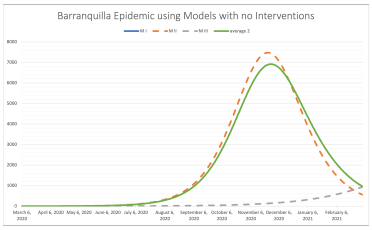

(c) Barranquilla model forecast

Figure 4: Comparison fitted ensemble model using the first three models (which are models with no interventions; see definition in Table 4).

magnitude than reported cases because it also included asymptomatic and pre-symptomatic cases along with symptomatic and reported cases. As an example, we also show (Figure 4) the averaging of ensemble models when specific types of the models are considered based on mechanisms captured in the models (see Table 4 for three different types of models categories).

We used a simple approach of averaging of ensemble models, however, there exists multiple other methods which are more sophisticated (Kulinich et al., 2020) such as Markov Chain ensemble (MCE) method, and Convex optimization (COE) method. For example, in the COE method, we compute a linear combination of the model outputs with $\omega_1, \omega_2, \ldots, \omega_N$ weights which minimizes mean squared differences with respect to observations:

$$\min_{\omega_j;\, j=1,\ldots,N} \sum_{t=1}^{T} (E_{COE_t} - O_t)^2 \qquad \text{s.t.} \quad E_{COE_t} = \sum_{j=1}^{N} \omega_j M_{j,t}, \qquad \sum_{j=1}^{N} \omega_j = 1 \quad \omega_j \geq 0$$

The trend bias of regular time periods is key quantity and can be calculated by taking the difference between the inclination parameter m in weighted ensembles and observations estimated using a linear function $y = m * x + b$ on validation data for each time period (suppose there are k time periods; it could be weekly, monthly or quarterly). The overall weighted ensemble trend bias is thus the mean of the trend biases for k different time periods.

5 Discussion

COVID-19 is a highly transmissible virus with the capacity to produce outbreaks and with high repercussions on lethality in the vulnerable (individuals with pre-health conditions or elderly) population and with comorbidities. Mathematical models and simulation applied to data ongoing epidemics allow anticipation in the phase of preparing mitigation plans. Based on the estimates of the model, the distribution of hospital beds and intensive care units in the city available for response to an eventual emergency have been planned. In this study, we highlight and present a use case for epidemic preparedness for Colombia and its five major cities. The goal here was to estimate location-dependent transmission rates, reproduction number, and disease burden using initial exponential growth of epidemics and provide robustness in the results via different types of models and ensemble modeling technique.

The estimates of R_0 here might be slightly lower (from 1.10 to 1.75) than those published by other studies (for example studies from Asia and Europe (Wu and McGoogan, 2020; Adhikari et al., 2020; Lauer et al., 2020)) but it could be due to lower density and reduced population mixing patterns in Colombia. We have observed the application of different techniques to calculate R_0, that could explain the different scenarios of a potential outbreak in Colombia. While Li et al. (2020) used the duration of the serial interval, whose result is similar to ours when we use the same technique, our highest estimate was based on the growth rate and the duration of similar pre-symptomatic and infectious periods. The pandemic in Colombia was recognized approximately 7 days after the arrival of the first case in the country, where estimated date of arrival was March 2, 2020. Among the 8 Latin American countries, Ecuador is estimated to have fastest initial exponential epidemic growth (0.26) and Panama the lowest growth rate (0.21) with Colombia growth rate (0.24) being in the middle of the list.

We compared model outcomes for five different cities of Colombia using averaging of ensemble models. The weights in the averaging of models in the ensemble were computed using error in fitting and number of estimated parameters. In the Models I–II, only one parameter (transmission rate) was estimated; whereas, in the Models III–V, two parameters were estimated and three parameters in Model VI (Table 8). Using error in the fit and number of estimated parameters, ensemble weights were computed and average model is generated. Using the ensemble technique, the simplest SIR model was found to be better fit to the data for the city of Cali; whereas, in the case of Bogota and Barranquilla, the dominant model was found to be SEIR model, which captured basic epidemiological characteristics (most infection driven by latently infected individuals) of COVID-19. The model with quarantine and isolation states was a best fit in case of Cartagena, showing that population followed prevention

policies better in this region. The complex model (Model VI) was not the preferred model in the ensemble for all the five cities of Colombia.

The present study shows a simple way of averaging the results from the model outcomes and using it to forecast outcomes with lower uncertainty than each of the model separately in the ensemble. However, as with any other study, our study also have a few limitations. The models considered were all single outbreak models and hence, were only meant to compare initial disease burden in the pandemic between cities. Moreover, the available limited data were only used to parameterized the model. In future, the work can be easily extended to include repeated peaks in an outbreak by modifying the models and incorporating features such as waning immunity, demographic parameters, or multiple strains.

Public health departments can tremendously benefit from the advance warning from the model based forecasts and prepare hospitals as well as alerting public of dangerously incoming epidemic surge. As shown here for the case of COVID-19 in Colombia, multi-model ensembles can effectively and simply aggregate models' predictions which are implemented under different epidemiological and structural differences. Thus, giving a tool to decision makers in a form of more accurate single aggregated prediction. Using such ensemble technique, public health departments can mitigate the full impact of an outbreak on a real time basis while providing effective adaptive public health policy, which is key in face of fast changing information on newly emerging diseases and its control. The ensemble technique is flexible and can rigorously capture disease trends that can support quick public health decision making and long lasting policy design.

Conflict of Interest Statement

Authors declare do not have any conflict of interest

References

Adhikari, S. P., S. Meng, Y. J Wu, Y. P. Mao, R. X. Ye, Q. Z. Wang, et al. (2020). Epidemiology, causes, clinical manifestation and diagnosis, prevention and control of coronavirus disease (COVID-19) during the early outbreak period: a scoping review. *Infectious Diseases of Poverty 9*(1), 1–12. doi: 10.1186/s40249-020-00646-x. 44, 53

Aeronáutica (2020). Pasajeros-Kilómetros (Miles) por principales rutas - Operación internacional. Aeronáutica Civil. Unidad Administrativa Especial. Ministerio del Transporte de Colombia. Available at: http://www.aerocivil.gov.co/atencion/estadisticas-de-las-actividades-aeronauticas/boletines-operacionales 42

Anaya, R. (2017). ¿Cómo aporta la aviación al desarrollo de la sociedad? *A21MX*. Available at: https://a21.com.mx/aeronautica/2017/10/05/como-aporta-la-aviacion-al-desarrollo-de-la-sociedad 42

Backer, J. A., D. Klinkenberg, and J. Wallinga (2020). Incubation period of 2019 novel coronavirus (2019-nCoV) infections among travellers from Wuhan, China, 20–28 January 2020. *Eurosurveillance 25*(5), 2000062. doi: 10.2807/1560-7917.ES.2020.25.5.2000062. 44

Brauer, F. and C. Castillo-Chavez (2012). *Mathematical models in population biology and epidemiology (Vol. 2)*. New York: Springer. 41, 48

Brauer, F. (2010). Epimedic Models I: Reproduction Numbers and the Final Size Relations. Accessed on April 15, 2020. Available at: https://www.fields.utoronto.ca/programs/scientific/10-11/drugresistance/emergence/fred1.pdf 46

Centers for Disease Control and Provention (2020). Interim Clinical Guidance for Management of Patients with Confirmed Coronavirus Disease (COVID-19). Available at: https://www.cdc.gov/coronavirus/2019-ncov/hcp/clinical-guidance-management-patients.html 44

Chaolin H., W. Yeming, and L. Xingwang (2020). Clinical features of patients infected with 2019 novel coronavirus in Wuhan, China. *The Lancet 395*(10223), 497–506. doi: 10.1016/S0140-6736(20)30183-5. 41, 43, 48

Chen, J. (2020). Pathogenicity and transmissibility of 2019-nCoV-a quick overview and comparison with other emerging viruses. *Microbes and Infection 22*, 69–71. doi: 10.1016/j.micinf.2020.01.004. 41, 42

Chen, T. M., J. Rui, Q. P. Wang, Z. Y. Zhao, J. A. Cui, and L. Yin (2020). A mathematical model for simulating the phase-based transmissibility of a novel coronavirus. *Infectious diseases of poverty 9*(1), 1–8. doi: 10.1186/s40249-020-00640-3. 44

COVID-19 (2020). COVID-19 CORONAVIRUS / CASES. Last updated: February 28, 2020, 16:30 GMT. https://www.worldometers.info/coronavirus/coronavirus-cases/ 42

Escobar, G. and D. M. Perilla (2019). *Cali en Cifras 2018-2019*. Departamento Administrativo de Planeación, Alcaldía de Santiago de Cali. Available at: https://www.cali.gov.co/documentos/1705/documentos-de-cali-en-cifras/ 42, 48

Figueroa, A. (2020). Científicos encuentran la nomenclatura definitiva para el nuevo coronavirus. *Notipress International*. México. 12 Febrero 2020. Available at: https://notipress.mx/internacional/cientificos-encuentran-la-nomenclatura-definitiva-nuevo-coronavirus-3099 41

Ganyani, T., C. Kremer, D. Chen, A. Torneri, C. Faes, J. Wallinga, and N. Hens (2020). Estimating the generation interval for COVID-19 based on symptom onset data. *medRxiv*. doi: 10.1101/2020.03.05.20031815 44

González-Jaramillo, V., N. González-Jaramillo, C. Gómez-Restrepo, O. H. Franco, C. A., Palacio-Acosta, and A. Gómez-López (2020). Proyecciones de impacto de la pandemia COVID-19 en la población colombiana, según medidas de mitigación. Datos preliminares de modelos epidemiológicos para el periodo del 18 de marzo al 18 de abril de 2020. *Revista de Salud Pública 22*, 1–6. doi: 0.15446/rsap.V22.85789. 44

Guan, W.-J., Z.-Y. Ni, Y. Hu, W.-H. Liang, C.-Q. Ou, J.-X. He, et al. (2020). Clinical characteristics of coronavirus disease 2019 in China. *New England Journal of Medicine 382*(18), 1708–1720. doi: 10.1056/NEJMoa2002032. 44

He, X., E. H. Y. Lau, P. Wu, X. Deng, J. Wang, X. Hao, et al. (2020). Temporal dynamics in viral shedding and transmissibility of COVID-19. *Nature Medicine 26*(5), 672–675. doi: 10.1038/s41591-020-0869-5. 44

Hu, Z., C. Song, C. Xu, G. Jin, Y. Chen, X. Xu, et al. (2020). Clinical characteristics of 24 asymptomatic infections with COVID-19 screened among close contacts in Nanjing, China. *Science China Life Sciences 63*(5), 706–711. doi: 10.1007/s11427-020-1661-4. 44

Huang, C., Y. Wang, X. Li, L. Ren, J. Zhao, Y. Hu, et al. (2020). Clinical features of patients infected with 2019 novel coronavirus in Wuhan, China. *The Lancet 395*(10223), 497–506. doi: 10.1016/S0140-6736(20)30183-5. 44

Imai, N., I. Dorigatti, A. Cori, S. Riley, and N. Ferguson (2020). Estimating the potential total number of novel Coronavirus cases in Wuhan City, China. *Imperial College London*, (17-01-2020). doi: 10.25561/77149. 44

Ivorra, B., M. R. Ferrández, M. Vela-Pérez, and A. M. Ramos (2020). Mathematical modeling of the spread of the coronavirus disease 2019 (COVID-19) taking into account the undetected infections. The case of China. *Communications in nonlinear science and numerical simulation 88*, 105303. doi: 10.1016/j.cnsns.2020.105303. 48

Kimball, A., K. M. Hatfield, M. Arons, A. James, J. Taylor, K. Spicer, et al. (2020). Asymptomatic and presymptomatic SARS-CoV-2 infections in residents of a long-term care skilled nursing facility – King County, Washington, March 2020. *Morbidity and Mortality Weekly Report 69*(13), 377–381. doi: 10.15585/mmwr.mm6913e1. 44, 48

Kucharski, A. J., T. W. Russell, C. Diamond, Y. Liu, J. Edmunds, S. Funk, and R. M. Eggo (2020). Early dynamics of transmission and control of COVID-19: a mathematical modelling study. *The lancet infectious diseases 20*(5), 553–558. doi: 10.1016/S1473-3099(20)30144-4. 48

Kulinich, M., Y. Fan, S. Penev, J. P. Evans, and R. Olson (2021). A Markov chain method for weighting climate model ensembles. *Geoscientific Model Development 14*(6), 3539–3551. doi: 10.5194/gmd-14-3539-2021. 53

Lauer, S. A., K. H. Grantz, Q. Bi, F. K. Jones, Q. Zheng, H. R. Meredith, et al. (2020). The incubation period of coronavirus disease 2019 (COVID-19) from publicly reported confirmed cases: estimation and application. *Annals of internal medicine 172*(9), 577–582. doi: 10.7326/M20-0504. 44, 53

Li, Q., X. Guan, P. Wu, X. Wang, L. Zhou, Y. Tong, et al. (2020). Early transmission dynamics in Wuhan, China, of novel coronavirus–infected pneumonia. *New England Journal of Medicine 382*, 1199–1207. doi: 10.1056/NEJMoa2001316. 42, 44, 48, 53

Liu, T., J. Hu, M. Kang, L. Lin, H. Zhong, J. Xiao, et al. (2020). Transmission dynamics of 2019 novel coronavirus (2019-nCoV). *Preprints with The Lancet*. doi: 10.2139/ssrn.3526307. 44, 48

Ministerio (2020). Información científico-técnica. Enfermedad por coronavirus, COVID-19. *Centro de Coordinación de Alertas y Emergencias Sanitarias*. Actualización: 28 de agosto 2020. Ministerio de Sanidad. Secretaría General de Sanidad y Consumo. Dirección General de Salud Pública, Calidad e Innovación. Accessed on September 15, 2020. Available at: https://www.mscbs.gob.es/profesionales/saludPublica/ccayes/alertasActual/nCov/documentos/ITCoronavirus.pdf 44

Mingwang S., P. Zhihang, X. Yanni, and Z. Lei (2020). Modelling the epidemic trend of the 2019 novel coronavirus outbreak in China. *bioRxiv* January 25, 2020. doi: 10.1101/2020.01.23.916726. 41

Mizumoto, K., K. Kagaya, A. Zarebski, and G. Chowell (2020). Estimating the asymptomatic proportion of coronavirus disease 2019 (COVID-19) cases on board the Diamond Princess cruise ship, Yokohama, Japan, 2020. *Eurosurveillance 25*(10), 2000180. doi: 10.2807/1560-7917.ES.2020.25.10.2000180. 44

MSE (2020). Informe Técnico, Nuevo coronavirus 2019-nCoV. Ministerio de Sanidad de España. *Centro de Coordinación de Alertas y Emergencias Sanitarias*. February 10, 2020. Available at: https://www.sempsph.com/images/ITCoronavirus.pdf 44

Mubayi, A., C. K. Zaleta, M. Martcheva, and C. Castillo-Chavez (2010). A cost-based comparison of quarantine strategies for new emerging diseases. *Mathematical Biosciences & Engineering 7*(3), 687–717. doi: 10.3934/mbe.2010.7.687. 48

Murcia (2020). Banco de Preguntas Preevid: Negativización del ARN viral en el paciente con COVID-19 leve. *Murciasalud*. Available at: http://www.murciasalud.es/preevid/23575 44

Nishiura, H., T. Kobayashi, T. Miyama, A. Suzuki, S. Jung, K. Hayashi, et al. (2020). Estimation of the asymptomatic ratio of novel coronavirus infections (COVID-19). *medRxiv*. doi: 10.1101/2020.02.03.20020248. 44

Oaks, S. C., Jr., R. E. Shope, and J. Lederberg (Eds.) (1992). *Emerging infections: microbial threats to health in the United States*. Washington, DC: National Academies Press. 42

Orellana, C. E. B., J. J. C. Chavez, C. Montalvo, J. Sullivan, E. Michael, and A. Mubayi (2020). Modeling and Preparedness: The Transmission Dynamics of COVID-19 Outbreak in Provinces of Ecuador. *medRxiv*. doi: 10.1101/2020.07.09.20150078. 48

Organización Mundial de la Salud (2020). Declaración sobre la segunda reunión del Comité de Emergencias del Reglamento Sanitario Internacional (2005) acerca del brote del nuevo coronavirus (2019-nCoV). 30 de enero de 2020. Ginebra, Suiza. Available at: https://www.who.int/es/news-room/detail/30-01-2020-statement-on-the-second-meeting-of-the-international-health-regulations-(2005)-emergency-committee-regarding-the-outbreak-of-novel-coronavirus-(2019-ncov) 41

Read, J. M., J. R. Bridgen, D. A. Cummings, A. Ho, and C. P. Jewell (2020). Novel coronavirus 2019-nCoV: early estimation of epidemiological parameters and epidemic predictions. *medRxiv*. doi: 10.1101/2020.01.23.20018549. 42

Tan, W., Y. Lu, J. Zhang, J. Wang, Y. Dan, Z. Tan, et al. (2020). Viral kinetics and antibody responses in patients with COVID-19. *medRxiv*. doi: 10.1101/2020.03.24.20042382. 44

Vynnycky, E. and R. White (2010). *An introduction to infectious disease modelling*. New York: Oxford University Press. 42

Wang, C., P. W. Horby, F. G. Hayden, and G. F. Gao (2020). A novel coronavirus outbreak of global health concern. *The Lancet 395*(10223), 470–473. doi: 10.1016/S0140-6736(20)30185-9. 44

Wei, W. E., Z. Li, C. J. Chiew, S. E. Yong, M. P. Toh, and V. J. Lee (2020). Presymptomatic Transmission of SARS-CoV-2—Singapore, January 23–March 16, 2020. *Morbidity and Mortality Weekly Report 69*(14), 411–415. doi: 10.15585/mmwr.mm6914e1. 48

Wu, Z. and J. M. McGoogan (2020). Characteristics of and important lessons from the coronavirus disease 2019 (COVID-19) outbreak in China: summary of a report of 72 314 cases from the Chinese Center for Disease Control and Prevention. *Jama 323*(13), 1239–1242. doi: 10.1001/jama.2020.2648. 44, 53

Zhao, S., Q. Lin, J. Ran, S. S. Musa, G. Yang, W. Wang, et al. (2020). Preliminary estimation of the basic reproduction number of novel coronavirus (2019-nCoV) in China, from 2019 to 2020: A data-driven analysis in the early phase of the outbreak. *International Journal of Infectious Diseases 92*, 214–217. doi: 10.1016/j.ijid.2020.01.050. 41

Zheng, J. (2020). SARS-CoV-2: An emerging coronavirus that causes a global threat. *International journal of biological sciences 16*(10), 1678–1685. doi: 10.7150/ijbs.45053. 44